Optimizing the operation of a photovoltaic generator by a genetically tuned fuzzy controller

NADIA DRIR, LINDA BARAZANE and MALIK LOUDINI

This paper presents design and application of advanced control scheme which integrates fuzzy logic concepts and genetic algorithms to track the maximum power point in photovoltaic system. The parameters of adopted fuzzy logic controller are optimized using genetic algorithm with innovative tuning procedures. The synthesized genetic algorithm which optimizes fuzzy logic controller is implemented and tested to achieve a precise control of the maximum power point response of the photovoltaic generator. The performance of the adopted control strategy is examined through a series of simulation experiments which prove good tracking properties and fast response to changes of different meteorological conditions such as isolation or temperature.

Key words: maximum power point tracking, P&O, styling, fuzzy control, genetic algorithms

1. Introduction

Renewable energy resources have enormous potential and can meet the present world energy demand. They can enhance diversity in energy supply markets, secure long-term sustainable energy supply, and reduce local and global atmospheric emissions. They can also provide commercially attractive options to meet specific requirements for energy services (particularly in developing countries and rural areas), and offer possibilities for local manufacturing of equipment [1]. One of the most promising renewable energy technologies is photovoltaic (PV) technology.

In order to extract at each moment of time the maximum power at the terminals of photovoltaic generator, an insertion of maximum power point tracker (MPPT) is necessary between the photovoltaic module and load. In literature we can find different techniques of tracking the MPP: perturb and observe method (P&O), the hill climbing method or the incremental conductance method. However, fast variations of atmospheric conditions (e.g. temperature and irradiation) showed the limitation of the conventional

_____

N. Drir and L. Barazane are with Faculté d'Electronique et d'Informatique, Université des Sciences et de la Technologie Houari Boumediene (USTHB), B.P. 32, El Alia, 16111 Bab Ezzouar, Algiers, Algeria. E-mails: dr_nadia22@hotmail.com, lbarazane@yahoo.fr. M. Loudini is with Ecole Nationale Supérieure d'Informatique, Laboratoire de Communication dans les Systèmes Informatiques B.P 68M, 16309 Oued Smar, El Harrach, Algiers, Algeria. E-mail: m_loudini@esi.dz

controller to track the MPP enough fast and with reduced output oscillations. This motivates searching for simple and robust controllers, possibly without the need for accurate mathematical description of the plant to be controlled.

This paper is focused mainly on application of alternative closed-loop intelligent control strategies, including fuzzy logic, which allow to obtain precise and robust control of the photovoltaic generator. For this purpose, an advanced control scheme resulting from the hybridization of a fuzzy logic based control scheme and genetic algorithm optimization is proposed.

The structure of the paper is as follows. In Section 2, a brief description of the overall model dynamics of the PV generator is presented. Section 3 is devoted to the theory of fuzzy logic and a presentation the simulation results of the fuzzy logic controller. In section 4, the basics of genetic algorithm optimization method is presented as well as derivation and description of the implementation issues of adopted smart control strategy. Before presenting the synthesized controller, the parameter adjustment of FLC are particularly highlighted. The performance of the resulting and genetically optimized fuzzy controller (GAOFLC) faced to different control tasks are examined through a series of simulation experiments. Concluding remarks are given in Section 6.
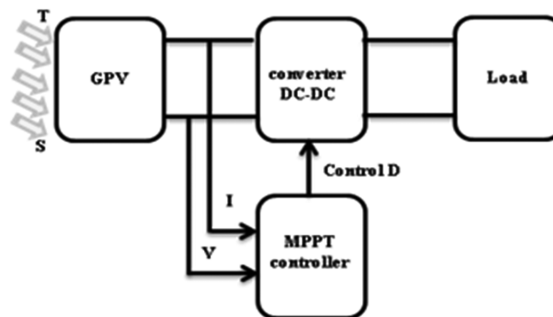

Figure 1. Photovoltaic system.

2. Photovoltaic power generation

Photovoltaic solar energy comes from direct conversion of a portion of solar radiation into electrical energy carried through a photovoltaic cell based on physical phenomenon called photovoltaic effect. The essence of this phenomenon is producing an electromotive force when the surface of the cell is exposed to the light [2]. The voltage generated varies a little what depends on a material used to manufacture the cell and differences of meteorological conditions.

Fig. 1 shows the complete block diagram of a PV module with a MPPT controller and feed power to the load through a DC/DC converter. Here, MPPT controller takes the output voltage (V) and current (I) of the PV module as its input and based on the control

algorithm it gives appropriate command to the converter to interface the load with the PV module.
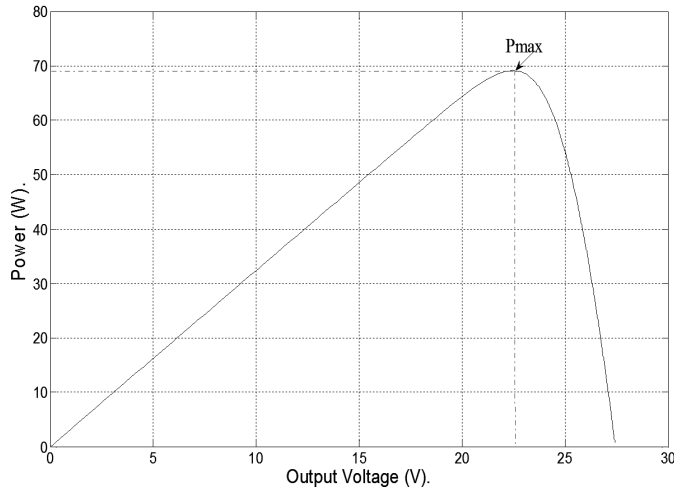

Figure 2. Power curve under constant irradiation and temperature.

As show in Fig. 2, in the power-voltage characteristic curve of photovoltaic generator, there is a maximum point called the maximum power point (MPP). With the varying atmospheric condition and because of the rotation of the earth [3], the irradiation and temperature keeps on changing throughout the day. This makes a great challenge to operate the PV module consistently on the maximum power point, thus number of MPPT algorithms have been developed [4]. In this paper, a fuzzy logic controller was used to control the unit.

3.   Fuzzy logic

Fuzzy logic was introduced in 1965 by L. Zadeh to formalize the representation and processing of imprecise or approximate knowledge to deal with systems of great complexity or unfamiliarity. Fuzzy logic is involved in the handling of imperfect knowledge, and it occurred as an effective alternative for such systems [5]. The concept of fuzzy logic comes from the observation that the Boolean variable, which can take only two values (true or false), is not well suited to the representation of the most common phenomena. Indeed, the classical logic considers that a proposal is either true or false. This helps to answer many situations, but in some cases a transition "abrupt" is embarrassing. In contrast, fuzzy logic distinguishes infinitely many truth values (between 0 and 1).

In standard set theory, an object is either a member of a set or it is not a member at all. Given an universe of objects U and a particular object $x \in U$, the degree or grade of membership $\mu_A(x)$ with respect to a set $A \subseteq U$ is:

$$\mu_A(x) = \begin{cases} 1 & \text{if} \quad x \in A \\ 0 & \text{if} \quad x \notin A \end{cases} \tag{1}$$

The function $\mu_A(x) : U \to \{0,1\}$ is called characteristic function in standard set theory. Often, a generalization of this idea is used, for instance, to handle data with error bounds. A degree of membership of one is assigned to all the numbers within some percent error, and all the numbers outside that interval a degree of membership of zero (Fig. 3-a). For the precise case, the membership degree is one at the exact number and zero everywhere else (Fig. 3-b)).
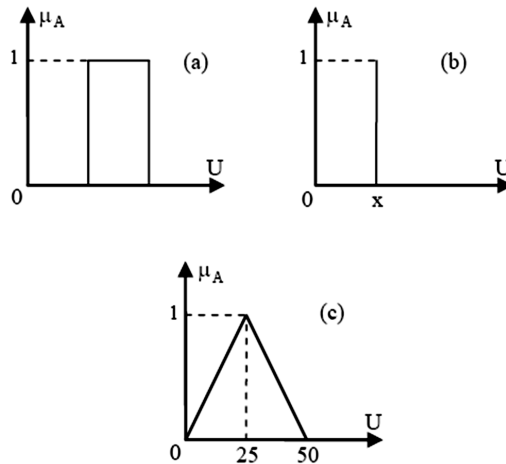

Figure 3. MFs for crisp and fuzzy data.

Zadeh [7] proposed a further generalization in which some objects are more member of set than others. The degree of membership takes on various values between zero and one, where a zero value indicates complete exclusion and a value of one indicates complete membership. This generalization expands the expressiveness power. For instance, to express that a temperature is around 25, we may use a triangular membership function (MF) (Fig .3-c) with its peak at 25 to express the idea that the closer a number is to 25 the better it qualifies.

The structure of a process controlled by the fuzzy controller is illustrated in Fig. 4, which emphasizes basic components of the fuzzy controller: fuzzification interface, a knowledge base, a data base, inference procedure, and a defuzzification interface. The basic constitutive components can be briefly presented as follows.
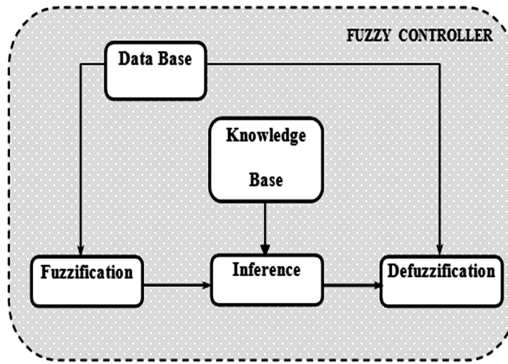
Figure 4. Basic structure of fuzzy logic control.

- The fuzzification interface gets the values of input variables, performs a scale mapping to transfer the range of values of input variables into corresponding universes of discourse, and performs the function of fuzzification to convert input crisp data into fuzzy values.

- The knowledge base comprises a rule base characterizing the control policy and goals.

- The data base provides the necessary definitions of discretization and normalization of universes, fuzzy partition of input and output spaces and MF definitions.

- The inference procedure process fuzzy input data and rules to infer fuzzy control actions employing fuzzy implication and the rules of inference in fuzzy logic.

- The defuzzification interface performs a scale mapping to convert the range of values of universes into corresponding output variables, and transformation of a fuzzy control action inferred into a nonfuzzy (crisp) control action.

3.1.   Fuzzy logic MPPT controller

The proposed fuzzy logic MPPT controller has two inputs and one output. Input variables are the error E and change of error ΔE defined as:

$$\begin{cases} E(n) = \dfrac{P(n) - P(n-1)}{V(n) - V(n-1)} \\ \Delta E(n) = E(n) - E(n-1) \end{cases} \tag{2}$$

where E and ΔE are the error and change in error, n is the sampled (discrete) time, $P(n)$ is the instantaneous power of the photovoltaic generator, and $V(n)$ is the corresponding instantaneous voltage. The input $E(n)$ shows the location of the load operation point

at the instant *n* on the left or on the right side of the maximum power point on the power-voltage characteristic, while the input $\Delta E(n)$ expresses the direction of this point moves. The output variable is the duty cycle *D*, which is transmitted to the boost DC/DC converter to drive the load.

The MPPT using the Mamdani FLC approach, which uses the min-max operation fuzzy combination law, is designed in a manner that the control task try to continuously move the operation point of the solar array as close as possible to the maximum power point (MPP) [15], and the defuzzification uses the center of gravity to compute the output of FLC. These two variables and the control duty cycle *D* used in presented application are illustrated in Fig. 5.
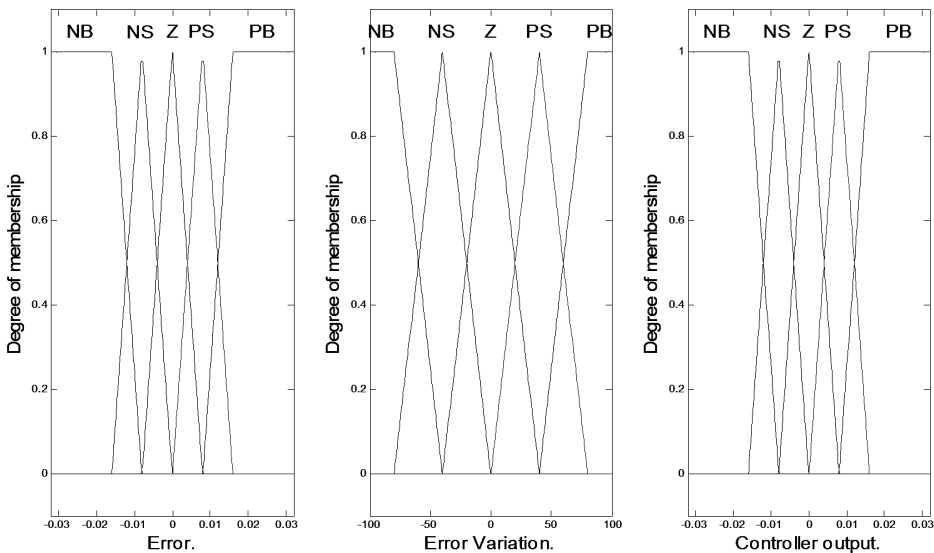

Figure 5. Membership functions of FLC.

Once the photovoltaic chain designed, and to verify the ability of presented fuzzy controller to improve the performance obtained under the conventional MPPT controller, numerical simulation was performed for different conditions as follows.

- Simulation of system operation under steady (standard) conditions: temperature of 25^0C and an irradiation of 1000W/m^2 (see Fig. 6).

- Simulations under varying conditions of temperature and irradiation (increasing the temperature from 20^0C to 45^0C, decreasing in sunlight from 1000 to 900 W/m^2 and increasing to 1000 W/m^2 in 2 seconds (see Fig.7).
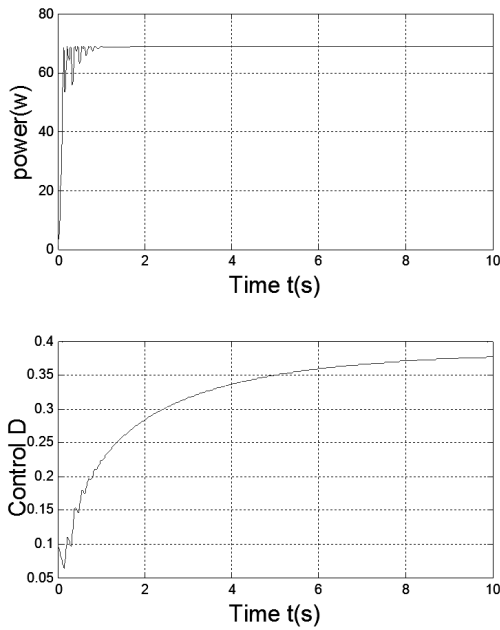
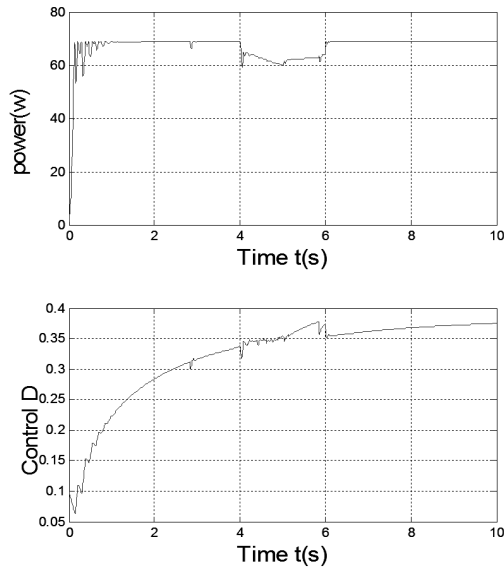Figure 6. FLC response for standard condition.

Figure 7. FLC response under varying conditions.

MPPT fuzzy logic controllers show good performance under varying atmospheric conditions. However, their effectiveness depends significantly on proper error computation and the rule base table. The application of the fuzzy controller has shown good ability to control the photovoltaic system. Further improvement can be obtained by optimizing fuzzy controller using meta-heuristics (genetic algorithm).

4. Brief review of genetic algorithms

Based on the Darwin's evolutionary theory [6], genetic algorithms (GA) were proposed by the computer scientist John Holland [7] as a general way of creating software solutions by evolutionary adaptive process. GA is a global search metaheuristic used to solve optimization problems.

The process that GA realizes (Fig. 8) consists of evolving an initial set of points, i.e. an initial population of randomly generated individuals (chromosomes) encoding solutions to the considered optimization problem to be solved towards final exact or approximate solutions. The process is executed by iterating a population with a constant size N.
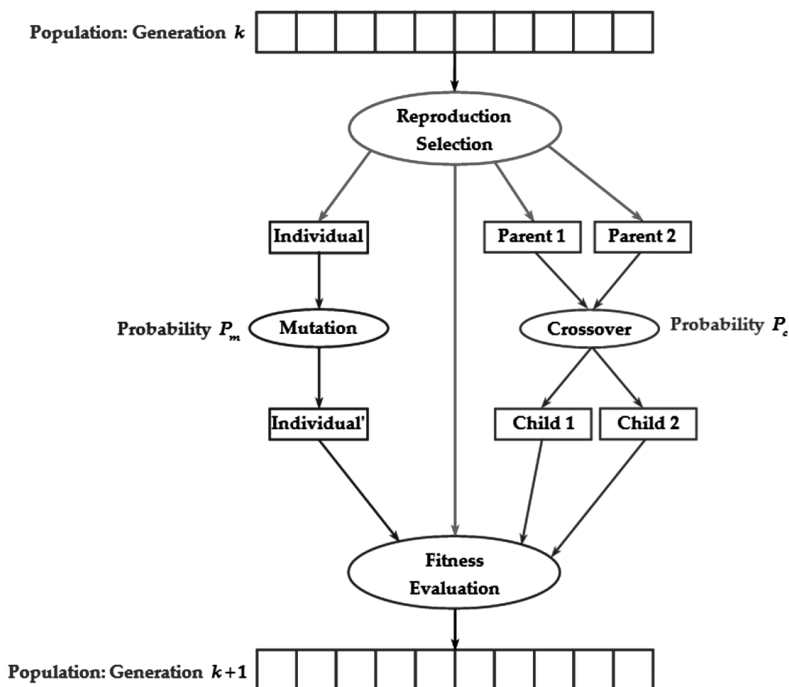

Figure 8. General principle of a genetic algorithm.

The evolution of the successive populations from the kth generation to the $(k + 1)$ bases on the operations of selection, crossover and mutation which are inspired by evolutionary biology [14]:

- Selection: A proportion of the population is selected among each of the successive generations to breed a new generation. The two mostly used and well-known selection methods are the *roulette wheel selection* and the *stochastic remainder without replacement selection*.

- Crossover: After the selection operation, the crossover operator reproduces new individuals from parents chosen with a probability P_c among the survived individuals. Three principle techniques are usually adopted: the *slicing crossover*, the *k-point slicing crossover*, and the *uniform crossover*.

- Mutation: This operation refers to a random change (mutation), with a probability P_m, in some selected chromosomes to escape local optima and to ensure accessibility of the entire solution space.

These operations or genetic operators act on all the kth generation individuals. For each generation, GA selects the best individuals according to an adaptation or a fitness which is the cost or optimization function.

The FLC is codified as a chromosome. GA optimization process starts with the first FLC as the initial solution and begins the iterative evaluation of the successively generated solutions by observing the objective (cost) function denoted by Of. This function is chosen to maximize the inverse of the well known and usually used performance index namely Integral of Time-weighted Absolute Error (ITAE) [5] abbreviated, here, as DITAE.

The mathematical expression for Of, minimized by the GA, can be written as:

$$Of = \frac{1}{DITAE} = \frac{1}{\sum\limits_{k=k_0}^{k=k_f} [kT_s \, |e\,(kT_s)|]} \tag{3}$$

where k_0 and k_f are the initial and final discrete times of the evaluating period and T_s is the sampling period.

In the literature it may be found different studies which uses GA to adjust parameter of the MPPT fuzzy controller like the structure of rules and membership functions [8]. Optimization of these two entities can be done separately, which may result in suboptimal solution, because the design parts are mutually dependent as is presented by Homaifar and McCormick (1995) who demonstrated clearly that by using GA to design both parameters simultaneously, the two elements of fuzzy controllers can be fully integrated to deliver a more finely tuned, high performance controller [9]. However, there are many other parameters that we can adjust to optimize FLC, other than the structure of rules and membership functions. In this work, GA is applied to automatically adjust the following FLC parameters:

- number of membership functions (MFs) for each FLC variable,

- MFs shapes for each FLC variable,

- MFs distribution for each FLC variable,

- decision table rules,

- scaling factors G_e, $G_{\Delta e}$, $G_{\Delta D}$.

In the next section, the assumptions and constraints introduced to simplify this process are explained in details.

4.1. Conception, hypotheses and constraints

Assumptions and constraints concerning decision table and FLC variables MFs to be optimized are as follows.

- The number of fuzzy sets (FSs) denoted as NFS for each variable can take only one of the following possible values: 3, 5, 7 or 9.

- The FSs are symbolized (labeled) by the standard linguistic designation and indexed in ascending order. If, for example, the number of FSs of a linguistic variable is equal to 7, the corresponding FSs can be: NB, NM, NS, ZE, PS, PM, PB and indexed from 1 to 7.

- The FSs NB, NM and NS are considered as the opposites to PB, PM and PS respectively (symmetrically with respect to ZE). The label ZE stands for linguistic (fuzzy) value zero, first letters N and P mean negative and positive and second letters B, M and S denote big, medium and small values respectively.

- All the FLC variables universes of discourses are normalized to the range $[-1,\ 1]$.

- The first and the last MFs have their apexes at -1 and +1 respectively.

4.2. Decision rules table deriving method

The method used for construction of decision rules table is inspired by [11] and [10] where sort of grid has been proposed. As the contribution, a new method of FSs assignment to each of the grid nodes in the special case of equality of distances between the points representing the candidate decision rules is proposed (see the decision rules table deriving method principle given below). Note that this new procedure is adopted instead of the random assignment proposed in [10].

A. *Principle of the method*

Firstly, the grid is constructed using two spacing parameters PSG_e and $PSG_{\Delta e}$ relatively to the FLC two inputs e and Δe.

The first (resp. the second) spacing parameter PSG_e (resp. $PSG_{\Delta e}$) fixes the grid nodes X-axis coordinates (resp. Y-axis coordinates) in the interval $[-1, 1]$ using a simple computing formula given in the next paragraph. Each abscissa (resp. ordinate) represents the FS according to the variable e (resp. Δe). The number of the grid constitutive nodes is then equal to the product of the two FLC input and FSs number.

Once the nodes are fixed, we introduce the output points on a straight line corresponding to the FLC output variable ΔD. Now, the points (output ones) represent the FSs but not their coordinates. The number of points is equal to the output variable FSs number. A third spacing parameter $PSG_{\Delta e}$ fixes the output points X-axis (Y-axis) coordinates similarly to the nodes fixing manner, whereas the Y-axis (X-axis) coordinates are calculated by the angular parameter, denoted as "$Angle$", which determine the slope of the straight line, supporting the output points, with respect to the horizontal axis. This angular parameter varies in the interval 0, $\pi/2$ counterclockwise.

Each of the grid nodes represents the case of the decision table and each output point represents the FS of the control variable ΔD.

Once all the points coordinates (grid nodes and output points) are determined, we can proceed to the assignment, by determining the minimal distance among all the distances separating each node of the grid from all the output points situated on the straight line. Then, we assign to each node of the grid the closest output point. Consequently, the decision table case corresponding to this node will contain the FS representing the selected output point.

Nevertheless, the assignment conflict could arise in the case of equality between two minimal distances separating a node and two output points. We propose to select the output point which has the lower FS index if it is a case of the upper part with respect to the table diagonal or the output point which has the greater FS index if the case belongs to the lower part. It should be noted that no more than two output points can be at the same distance from a given node of the grid since all the output points are on the same straight line.

B. *Spacing parameter*

The grid spacing parameter *PSG* specifies how the positions C_i of the intermediate points (between the center and the extreme of each graduated axis) are spaced out with respect to the central point. This parameter offers a flexibility of varying spacing. The more it is greater than 1, the more the points positions are closed to the center and vice versa. At the value 1, the positions are uniformly distributed in the universe of discourse interval $[-1, 1]$. The number of positions C_i and FSs are, obviously, the same, thus we have proposed a formulation of the spacing law in function of the spacing parameter *PSG*.

At a first stage, the positions C_i being equidistant are denoted by CEq_i and computed as

$$CEq_i = 2 \left(\frac{i-1}{NEF-1} \right) - 1, \quad i = 1, \cdots, NFS. \tag{4}$$

Table 1. C_i in function of PSG for 7 FSs.

PSG	C_i						
	C_1	C_2	C_3	C_4	C_5	C_6	C_7
0.25	-1	-0.90	-0.76	0	0.76	0.90	1
0.5	-1	-0.81	-0.58	0	0.58	0.81	1
1	-1	-0.67	-0.33	0	0.33	0.67	1
2	-1	-0.44	-0.11	0	0.11	0.44	1
4	-1	-0.20	-0.01	0	0.01	0.2	1

Table 2. Constructing parameters of the illustrative example.

NFS_e	$NFS_{\Delta e}$	$NFS_{\Delta D}$	PSG_e	$PSG_{\Delta e}$	$PSG_{\Delta D}$	$Angle$
5	5	5	0.5	1	2	30^0

The C_i values are then determined in terms of the spacing parameter CE_i as follows

$$C_i = \text{sign}(CEq_i)|CEq_i|^{PSG} \tag{5}$$

where

$$\text{sign}(x) = \begin{cases} 1 & \text{if } x \geqslant 0 \\ -1 & \text{if } x < 0 \end{cases} \tag{6}$$

and $PSG = (PSG_1)^{PSG_2}$ with PSG_2 is equal to 1 or -1. An illustrative example of C_i computation is given in Tab. 1 for 7 FSs with different values of the spacing parameter.

To understand the decision table deriving procedure, a detailed example is given bellow. The constructing parameters are given in Tab. 2, then, the grid and the corresponding decision table are shown in Fig. 9.

It is interesting to note that the decision table obtained for $PSG_e = PSG_{\Delta e} = PSG_{\Delta D} = 1$ and $Angle = 45^0$ is the same as Mac Vicar-Whelan diagonal table [13].

4.3. Membership functions deriving method

Determination of the FLC MFs using the GA takes place in three phases as follows.

1. creation of primary MFs of the FLC input/output parameters,

2. parameterization,

3. adjustment of the MFs.

(a)
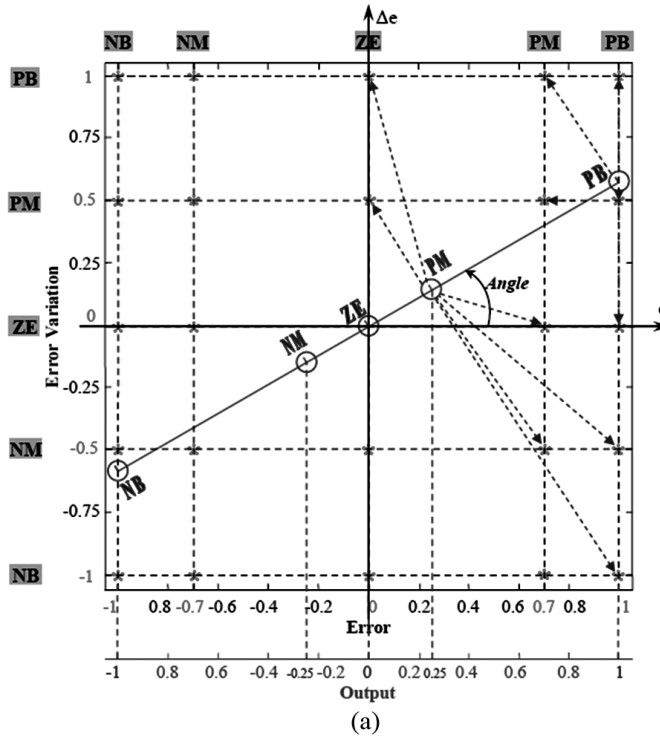
ΔD		e				
		NB	NM	ZE	PM	PB
	NB	NB	NB	NM	ZE	PM
	NM	NB	NB	NM	PM	PM
Δe	ZE	NB	NM	ZE	PM	PB
	PM	NM	NM	PM	PB	PB
	PB	NM	ZE	PM	PB	PB

(b)

Figure 9. Decision table deriving procedure example: (a) Grid constitution for decision table construction. (b) Derived decision table.

A. *MFs shape and width optimization*

Three types of MF shapes are considered:

- triangular,
- trapezoidal which include (generalize) the triangular one,

- "two-sided" Gaussian with flattened summit.

The triangular shape is defined by three parameters $\begin{bmatrix} P1 & P2 & P3 \end{bmatrix}$ representing, respectively, the left abscissa of the triangle base, the peak abscissa, and the right abscissa of the triangle base. Each triangle base begins at the precedent triangle peak abscissa and ends at that of the following one.

Trapezoidal shape is defined by four parameters $\begin{bmatrix} P1 & P2 & P3 & P4 \end{bmatrix}$ representing, respectively, the base left abscissa, the summit left abscissa, the summit right abscissa, and the base right abscissa. It is, then, framed by four points with the coordinates: $(P1,0)$, $(P2,1)$, $(P3,1)$ and $(P4,0)$ (see Fig. 10). Note that if $P2 = P3$, we obtain the triangular shape.

We also define two-sided Gaussian shape using four parameters $\begin{bmatrix} Sig1 & G1 & G2 & Sig2 \end{bmatrix}$ (see Fig. 11). The left and right sides of the Gaussian function are respectively defined by: $G(x) = e^{-\frac{(x-G1)^2}{2(Sig1)^2}}$ and $G(x) = e^{-\frac{(x-G2)^2}{2(Sig2)^2}}$.
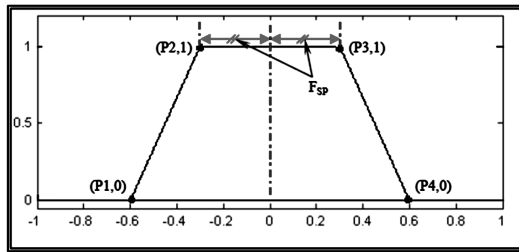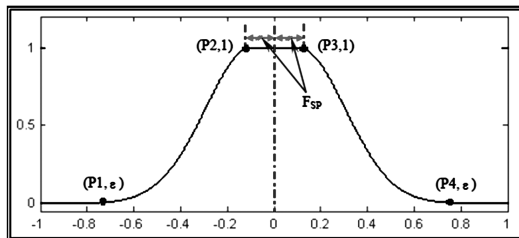

Figure 10. Trapezoidal MF.

Figure 11. Two-sided Gaussian MF.

To be able to use this two-sided Gaussian shape within the framework of our optimizing method, we need to constrain this shape by the same points used for the trapezoidal shape. In other words, we must define two-sides Gaussian shape in terms of the parameters $\begin{bmatrix} P1 & P2 & P3 & P4 \end{bmatrix}$ instead of $\begin{bmatrix} Sig1 & G1 & G2 & Sig2 \end{bmatrix}$. For that purpose, we adopt a very small positive real number ε (e.g. $\varepsilon = 0.01$ is suitable) such as:

- The Gaussian left curve includes the points $(P1, \varepsilon)$ and $(P2, 1)$,

- The Gaussian right curve includes the points $(P3, 1)$ and $(P4, \varepsilon)$.

This formulation allows to establish the following two systems of equations:

$$
\begin{cases}
e^{-\frac{(P1-G1)^2}{2(Sig1)^2}} = \varepsilon \\
e^{-\frac{(P2-G1)^2}{2(Sig1)^2}} = 1
\end{cases}
\qquad
\begin{cases}
e^{-\frac{(P3-G2)^2}{2(Sig2)^2}} = 1 \\
e^{-\frac{(P4-G2)^2}{2(Sig2)^2}} = \varepsilon
\end{cases}
\tag{7}
$$

The resolution of (7) gives: $G1 = P1$, $G2 = P3$, $Sig1 = \sqrt{-\frac{(P1-P2)^2}{2\log\varepsilon}}$ and $Sig2 = \sqrt{-\frac{(P4-P3)^2}{2\log\varepsilon}}$. Note that ε has been used since the two sides of the Gaussian function never pass by a null abscissa.

B. *Width spacing parameter*

The summits abscissae of the different shapes are calculated with the same principle of parameter spacing used in the determination of the grid nodes and points coordinates for the decision table derivation. The FLC input/output variables MFs spacing parameters are, respectively, denoted by PSF_e, $PSF_{\Delta e}$ and $PSF_{\Delta D}$.

C. *Shape optimizing parameter*

The MFs spacing method is inspired by [11, 10, 12]. In this paper we propose, a new technique for the MFs shape optimization. It is based on a design parameter called shape parameter (SP). This parameter allows for diversification (hybridization) of MFs shapes on the universe of discourse of each of the FLC input/output variables. SP is considered as a real number from the interval [0, 2]. Its integer part, denoted by I_{SP}, determines the shape of the MF. Its fractional part, denoted by F_{SP}, determines the spacing with respect to the center of the MF.

The MF shape is specified by I_{SP} and F_{SP} as follows:

- $I_{SP} = 0$: trapezoidal or triangular shape,

- $I_{SP} = 1$: two-sided Gaussian shape,

- F_{SP} determines the symmetric space with respect to the center of the MF as shown in Fig. 10 and Fig. 11. I follows from Fig. 10, that if the spacing is equal to zero, the trapezoidal shape reduces to the triangular one.

The number of MFs (NFS) for each one of the FLC input/output variables being optimized by GA is not constant. Consequently, it is not conceivable to allocate a spacing

parameter to each MF. For that purpose, we propose a solution which consists in allocating a shaping parameter, denoted by SP_M, for the MF in the middle of the universe of discourse and another, denoted by SP_E, for the extreme MF.

The intermediate MFs shaping parameters, denoted by SP_I, are then deducted from SP_M and SP_E so that they will have equidistant intermediate values. The ith shape parameter $SP_I(i)$ corresponding to the ith intermediate MF is determined by:

$$SP_I(i) = SP_M + 2(i-1)\frac{SP_E - SP_M}{NFS - 1}, \quad i = 1, \ldots, \frac{NFS + 1}{2} \tag{8}$$

We can observe that $SP_I(1) = SP_M$ and $SP_I\left(\frac{NFS+1}{2}\right) = SP_E$. So, only two parameters are enough for any number of FSs.

The previous MF shaping parameters are allocated to the FLC three variables e, Δe and ΔD as follows:

- $SP_M e$, $SP_M \Delta e$ and $SP_M \Delta D$,

- $SP_E e$, $SP_E \Delta e$ and $SP_E \Delta D$,

- $SP_I e$, $SP_I \Delta e$ and $SP_I \Delta D$.

Note that if the MFs shaping parameters of middle and extremity are equal, all the universe of discourse MFs will have the same shape generated by these parameters. It is also important to prevent important overlapping between the generated MFs which is undesirable in fuzzy control (flattening phenomenon) [12]. For this purpose, we have fixed a maximum value of F_{SP} to the half of the minimal distance between the two neighboring summits.

4.4. Parameter encoding

To run GA, a suitable encoding for each of the optimizing parameters is specified in terms of variation range, precision step and number of bits. We use a binary encoding for a more accurately solution space exploration.

5. Application of the GAOFLC

The GAOFLC based photovoltaic generator control architecture is shown in Fig. 12.

The algorithm for FLC optimal tuning based on GA method is applied and the resulting controller parameters are set. During the search process, GA looks for the optimal setting of the FLC parameters which maximize the cost function Of. Solutions with low DITAE are considered best suited. After many tests, we have adopted the parameter encoding shown in Tab. 3.

Many series of executions have been performed with variation of all GA parameters (mainly population size, selection routine, crossover method, crossover and mutation
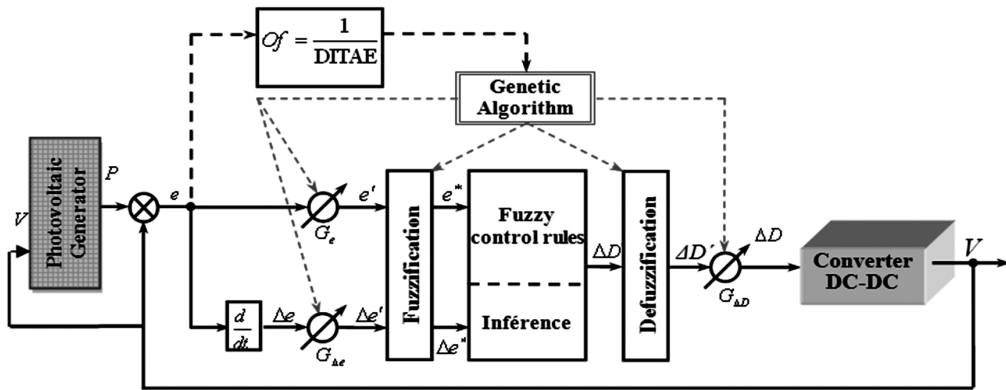
Figure 12. GAOFLC based feedback control system architecture.

Table 3. Parameters adopted for encoding.

Parameter	Interval	Precision	Number of encoding bits
NFS	$[3, 9]$	2	2
PSG_1	$[0.1, 1]$	0.01	7
PSG_2	$[-1, 1]$	2	1
$Angle$	$[0, \pi/2]$	$\pi/512$	9
PSF_1	$[0.1, 1]$	0.01	7
PSF_2	$[-1, 1]$	2	1
SP	$[0, 1.99]$	0.01	8
$G_e, G_{\Delta e}$	$[0, 50]$	0.01	13
$G_{\Delta D}$	$0, 50]$	0.1	9

probabilities). After the optimization process, the best result has been obtained for $Of = 2.0663$ ($DITAE = 0.48$).The corresponding GA characteristics are illustrated by Tab. 4. The GAOFLC design parameters and its main characteristics (MFs and decision table) are shown in Tab. 5, Fig. 13 and Tab. 6.

In the following, the derived GAOFLC is employed in different simulated control tasks concerning precise, robustness and stability of the maximum power point.

The first test is devoted to compare the performance of the designed GAOFLC controller and the conventional P&O tracker in a standard condition: solar irradiation was 1000 W/m^2 and temperature was 25^{0}C. Fig. 14 shows the result of power tracking obtained by these two controllers. It can be seen, that GAOFLC is faster then the con-

Table 4. GA adopted parameters.

Population size	25
Number of generations	3
Selection method	roulette wheel selection
Crossover method	1-point slicing crossover
Crossover probability	0.9
Mutation probability	0.1

Table 5. GAOFLC design parameters.

$NFS_e, NFS_{\Delta e}, NFS_{\Delta D}$	3, 9, 3
$PSG_e, PSG_{\Delta e}, PSG_{\Delta D}$	0.77, 0.27, 0.5
$Angle$	0.2218 rad
$PSF_e, PSF_{\Delta e}, PSF_{\Delta D}$	0.37, 0.5, 0.7
$SP_M e, SP_M \Delta e, SP_M \Delta D$	0.28, 0.73, 0.72
$SP_E e, SP_E \Delta e, SP_E \Delta D$	1.89, 0.84, 1.78
$G_e, G_{\Delta e}, G_{\Delta D}$	-0.079, -0.46, 1

Table 6. Decision table of the GAOFLC.

D		Δe								
		NB	NM	NS	NVS	Z	PVS	PS	PM	PB
e	NB	NB	NB	NB	NB	NB	NB	NB	NB	NB
	Z	Z	Z	Z	Z	Z	Z	Z	Z	Z
	PB	PB	PB	PB	PB	PB	PB	PB	PB	PB

ventional P&O tracker. Moreover the P&O based controller presents oscillations before achieving the MPP.

Next simulation was performed under rapid variation of solar irradiation (from 1000 W/m^2 to 850 W/m^2 through 900 W/m^2 and change back from 850 W/m^2 to 950 W/m^2 in 0.1s). The result of control is shown in Fig. 15. Then, the GAOFLC was tested for rapid variation of temperature (increasing the temperature from 25^{0}C to 35^{0}C in 0.1s and decrease from 35^{0}C to 25^{0}C in 1s), see Fig. 16.
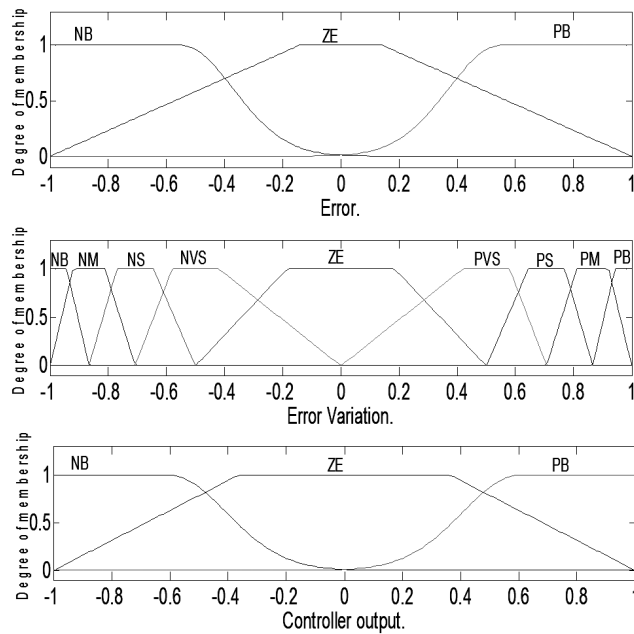
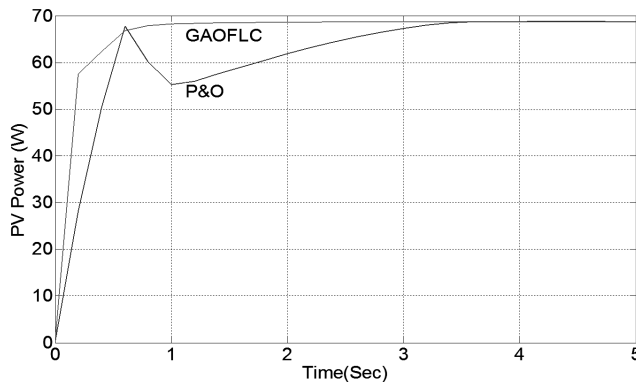Figure 13. Membership functions of the GAOFLC.

Figure 14. Provided power from P&O tracker and GAOFLC controller.

It can be clearly seen, that the system presents no overshoot and the maximum power point is well monitored by the controller in different condition.

Last simulation was performed under varying conditions of temperature and irradiation (irradiation from 1000 W/m^2 to 1200 W/m^2 and change back from 1200 W/m^2 to 1000 W/m^2 in 0.1s and temperature increasing from 25^{0}C to 35^{0}C in 0.1s – see Fig. 17).
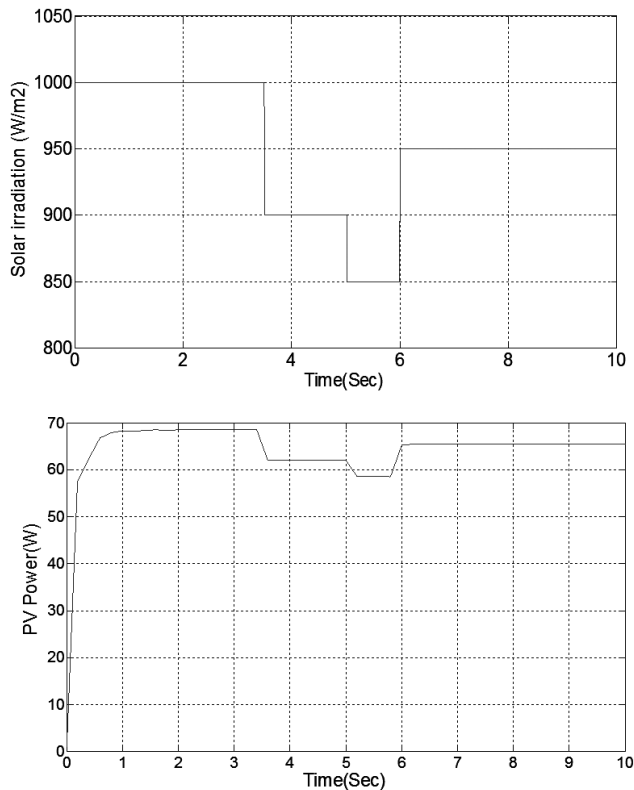
Figure 15. Output power of PV for different irradiation.

It can be seen, that GAOFLC tracker behaves properly for different variations considered.

6. Conclusion

This paper describes study of synthesis and application of an advanced control scheme based on fuzzy logic concepts and genetic algorithm optimization. This concept was applied to control PV systems, in order to track the MPP under different temperature and irradiation conditions.

Genetic algorithms are well known to be a powerful search tools that can reduce time and effort involved in designing systems for which no systematic design procedure exists. GA have been used here to build an optimized fuzzy logic controller for PV systems. GA have been used with success in this work, to enhance performance of a fuzzy logic based MPPT controller by optimizing simultaneously: number of membership functions
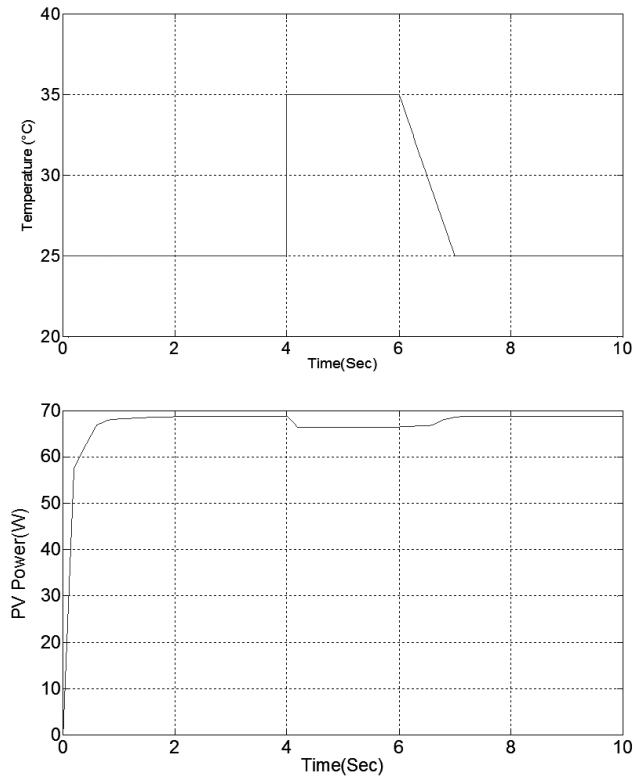
Figure 16. Output power of PV for different temperature.

(MFs) for each FLC variable, MFs shapes for each FLC variable, MFs distribution for each FLC variable, decision table rules and scaling factors G_e, $G_{\Delta e}$ and $G_{\Delta D}$.

The resulting optimized controller (GAOFLC) showed satisfactory performance in terms of speed and precision of power point maximum tracking in different atmospheric conditions without fluctuations of steady state.

References

[1] M. ASIF and T. MUNEER: Energy supply, its demand and security issues for developed and emerging economies. *Renewable Sustain Energy Rev.*, **11**(7), (2007), 1388-1413.

[2] M. ANGEL CID PASTOR: Conception et réalisation de modules photovoltaiques électroniques. Thèse de doctorat, Institut National des Sciences Appliquées, Toulouse, France, 2006.
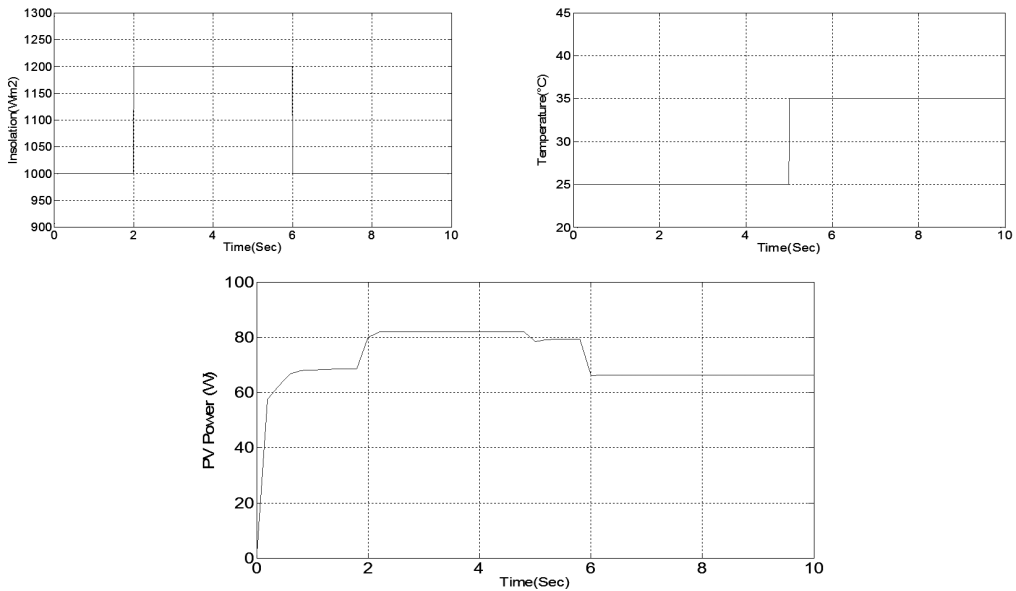
Figure 17. GA MPPT response under varying condition of temperature and irradiation.

[3] P.S. REVANKAR, W.Z. GANDHARE and A.G. THOSAR: Maximum power point tracking for PV systems using MATALAB/SIMULINK. *In Proc. Second Int. Conf. on Machine Learning and Computing (ICMLC)*, Bangalore, India, (2010), 8-11.

[4] T. ESRAM and P.L. CHAPMAN: Comparison of photovoltaic array maximum power point tracking techniques. *IEEE Trans. on Energy Conversion*, **22**(2), (2007), 439-449.

[5] D. GRAHAM and R.C. LATHROP: The synthesis of optimum transient response: criteria and standard forms. *Trans. of the American Institute of Electrical Engineers*, Part 2: Applications and Industry, **72** (1953), 273-288.

[6] C. DARWIN: On the origin of species by means of natural selection or the preservations of favoured races in the struggle of life. John Murray, 1859.

[7] J.H. HOLLAND: Adaptation in natural and artificial systems. Ann Arbor, MI, Univ. Michigan Press, 1975.

[8] C. LARBES, S.M. AIT CHEIKH, T. OBEIDI and A. ZERGUERRES: Genetic algorithms optimized fuzzy logic control for the maximum power point tracking in photovoltaic system. *Renewable Energy*, **34**(10), (2009), 2093-2100.

[9] A. MESSAI, A. MELLIT, A. GUESSOUM and S.A. KALEGIROU: Maximum power point tracking using a GA optimized fuzzy logic controller and its FPGA implementation. *Solar Energy*, **85**(2), (2011), 265-277.

[10] J. FORAN: Optimisation of a fuzzy logic controller using genetic algorithms. Master of Engineering Project Report, School of Electronic Engineering, Dublin City University, 2002.

[11] Y.J. PARK, H.S. CHO and D.H. CHA: Genetic algorithm-based optimization of fuzzy logic controller using characteristic parameters. *In Proc. IEEE Int. Conf. on Evolutionary Computation (ICEC 1995)*, Perth, WA, Australia, (1995), 831-836.

[12] H. BÜHLER: Réglage par logique floue. Presses Polytechniques et Universitaires Romandes, Lausanne, Switzerland, 1994.

[13] P.J. MAC VICAR-WHELAN: Fuzzy sets for man machine interactions. *Int. J. of Man Machines Studies*, **8**(6), (1976), 687-697.

[14] D.E. GOLDBERG: Genetic algorithms in search, optimization and machine learning, Addison Wesley, 1989.

[15] N. KHAEHINTUNG, K. PRAMOTUNG, B. TUVIRAT and P. SIRISUK: RISC-microcontroller built-in fuzzy logic controller of maximum power point tracking for solar-powered light-flasher applications. Dept. of Control & Instrum. Eng, Mahanakorn University of Technology, Bangkok, Thailand, 2004.